DYNAMIC BEHAVIOR OF GROUNDING GRIDS

L. Grcev
Eindhoven University of Technology, Eindhoven, The Netherlands[1]
(leonid.grcev@ieee.org)

Abstract: This paper presents an analysis of the dynamic behavior of grounding grids applying electromagnetic field method. Computer software is used to analyze spatial and temporal distributions of voltage to ground of grounding grid conductors presented in 3D graphical form as a sequence of snapshots of computer animation. The results of computations are validated by comparison with experimental works. Behavior in the first μs of the lightning impulse is analyzed, that is, when the transient processes are most intense. A number of cases are analyzed to illustrate the influence of the different parameters. It is demonstrated that circuit based models are not capable for such analysis.

1. Introduction

Extended meshed networks of buried conductors, the grounding grids, are considered as the most effective solution for grounding of large substations and plants. Their primary goal during abnormal conditions, such as power system faults and lighting strikes, is to ensure safety and also to prevent damage of equipment. They also provide common reference voltage to all interconnected electrical and electronic systems. While these goals are usually ensured at 50/60 Hz, the situation is quite different when impulsive currents, such as in case of lightning strike, are discharged into the earth. From the moment when the impulsive currents are injected in the grounding grid, uneven distributions of currents cause disturbances, which may provoke malfunction and destruction of components in connected electrical and electronic systems. Such disturbances during the transient period may be usually attributed to the local inequalities of the reference voltage and the electromagnetic induction. Knowledge of the spatial and temporal distributions of such voltages on the grounding systems in case of lightning strikes is of interest in EMC studies.

The problem of modeling the dynamic behavior of grounding grids attracts considerable interest, according to a number of recent publications (please see for example [1-12]). The models may be classified in following broad categories:

1. Engineering models [1,2,3],
2. Circuit models (with concentrated and distributed parameters) [4,6,10,11,12],
3. Hybrid models [5], and
4. Electromagnetic field models [7,8,9].

However, there is no consensus on the validity of different methodologies, on the domains of their applicability and their validation. This is especially true for the more simplified models (in categories 1 to 3 above), which are often used out of their applicability domain. An example of the later is pointed out in Section 4 of this paper.

This paper presents an analysis of the dynamic behavior of grounding grids applying electromagnetic field method. Computer software is used to analyze spatial and temporal distributions of voltage to ground of grounding grid conductors presented in 3D graphical form as a sequence of snapshots of computer animation. The results of the computations are validated by comparison with reliable and carefully documented independent experimental works [13,14]. Finally, results are presented to analyze behavior in the first μs of the lightning impulse, that is, when the transient processes are usually most intense. A number of cases are analyzed to illustrate the influence of the following parameters:

1. location of feed point and current impulse front time,
2. soil conductivity,
3. grounding grid size, and,
4. conductor separation.

2. Electromagnetic field method

The electromagnetic field approach describes the problem in frequency domain rigorously applying the full set of Maxwell's equations with the minimum possible neglects. An estimation of the overvoltages in power systems, however, can effectively be performed in time domain. For such purpose the electromagnetic field approach is interfaced to EMTP [9]. In a stand-alone simulation, such as in this paper, this can be achieved by an inverse Fourier-transform [7,8]. In case when impulses continue for long times, modified Fourier-transform may be used [15].

2.1 Basic assumptions

The model is based on the following assumptions [7]:

1. The earth and the air are homogeneous and occupy half-spaces with a common horizontal plane boundary between them.
2. The earth and the grounding electrodes exhibit linear and isotropic characteristics: conductivity, permittivity and permeability.
3. The grounding systems are modeled as networks of arbitrary oriented cylindrical metallic conductors. They are assumed to be subject to the thin-wire approximation, i.e., the ratio of the length of the conductor segment to its radius is $\gg 1$.

2.2 The mathematical model

For simplicity we will restrict our analysis to horizontal grounding grids. The total electric field $\mathbf{E}$ in the ground can be considered as the sum of an impressed electric field $\mathbf{E}^i$ the scattered electric field $\mathbf{E}^s$ due to the currents and charges induced in the grounding system electrodes by the impressed electric field. (Bold letters denote vectors and ^ unit vectors throughout the text.) Stating the boundary condition for the tangential component of the electric field derives the expres-

[1] On leave from St. Cyril and Methodius University, Skopje, Macedonia

sion for the induced currents and charges. The equation requires only the axial components because of the thin-wire approximation:

$$\hat{\mathbf{t}} \cdot \left(\mathbf{E}^i + \mathbf{E}^s \right) = 0 \tag{1}$$

Let the position of the electric dipole $I(\mathbf{r}')d\boldsymbol{\ell}$ at the conductor axis ℓ' be denoted by $\mathbf{r}'$, and the position at the conductor surface by $\mathbf{r}$, where $d\boldsymbol{\ell}' = \hat{\boldsymbol{\ell}}' \mathrm{d}\ell'$. The electric field vector $\mathbf{E}^s(\mathbf{r})$ is expressed in terms of magnetic vector potential $\mathbf{A}(\mathbf{r})$ and electric scalar potential $\phi(\mathbf{r})$

$$\mathbf{E}^s(\mathbf{r}) = -\nabla\phi(\mathbf{r}) - j\omega\mathbf{A}(\mathbf{r}) \tag{2}$$

which could be represented in integral form by

$$\mathbf{A}(\mathbf{r}) = \overline{\boldsymbol{G}}_A(\mathbf{r}|\mathbf{r}') \cdot I(\mathbf{r}')d\boldsymbol{\ell}' \tag{3}$$

$$\phi(\mathbf{r}) = G_\phi(\mathbf{r}|\mathbf{r}')q(\mathbf{r}')d\ell \tag{4}$$

$$q = \frac{-1}{j\omega}\nabla' I \tag{5}$$

Here the integration is carried along the axis ℓ of the grounding system electrodes. The time-variation exp($j\omega t$) has been suppressed throughout this paper. Also here, G_ϕ is the scalar potential Green's function and $\overline{\mathbf{G}}_A$ is dyadic Green's function of the magnetic vector potential:

$$\overline{\boldsymbol{G}}_A = (\hat{\mathbf{x}} \cdot \hat{\mathbf{x}} + \hat{\mathbf{y}} \cdot \hat{\mathbf{y}})G_{xx}^A + \hat{\mathbf{z}} \cdot \hat{\mathbf{x}} G_{zx}^A + \hat{\mathbf{z}} \cdot \hat{\mathbf{y}} G_{zy}^A \tag{6}$$

When the source and observation points are in the ground (medium 1), the spatial domain Green's functions are:

$$G_{xx}^A = \frac{\mu_0}{4\pi}\left[G_d + S_0\left(\frac{\gamma_1 - \gamma_0}{\gamma_1(\gamma_1 + \gamma_0)} \right) \right] \tag{7}$$

$$G_{zx}^A = \frac{-\mu_0}{4\pi}\frac{\partial}{\partial x} S_0\left(\frac{k_1^2\gamma_0 - k_0^2\gamma_1}{\lambda^2\left(k_1^2\gamma_0 + k_0^2\gamma_1\right)} - \frac{\gamma_1 - \gamma_0}{\lambda^2(\gamma_1 + \gamma_0)} \right) \tag{8}$$

$$G_{zy}^A = \frac{-\mu_0}{4\pi}\frac{\partial}{\partial y} S_0\left(\frac{k_1^2\gamma_0 - k_0^2\gamma_1}{\lambda^2\left(k_1^2\gamma_0 + k_0^2\gamma_1\right)} - \frac{\gamma_1 - \gamma_0}{\lambda^2(\gamma_1 + \gamma_0)} \right) \tag{9}$$

$$G_\phi = \frac{1}{4\pi\varepsilon_1}\left[G_d + \frac{k_1^2 - k_0^2}{k_1^2 + k_0^2} G_i + k_1^2 S_0\left(\frac{2k_1^2(\gamma_1 - \gamma_0)}{\gamma_1\left(k_0^2\gamma_1 + k_1^2\gamma_0\right)} \right) \right] \tag{10}$$

$\gamma_i = \sqrt{\lambda^2 - k_i^2}$, i = 1 (ground) and i = 0 (air)

$k_0^2 = \omega^2\mu_0\varepsilon_0$, $k_1^2 = \omega^2\mu_0\varepsilon_1$, $\varepsilon_1 = \varepsilon_0\varepsilon_{r1} - j\sigma_1/\omega$

Here S_0 is Sommerfeld-type integral of the form:

$$S_0(f) = \int_0^\infty f(\lambda) e^{-\gamma_1|z+z'|} J_0(\lambda\rho)\lambda d\lambda \tag{11}$$

where J_0 is the Bessel function of order zero, ρ is radial distance from source to observation point, and ε_{r1} and σ_1 are relative permittivity and conductivity of the soil, respectively. Here also:

$$G_d = \exp(-jk_1r_1)/r_1 \text{ and } G_i = \exp(-jk_1r_2)/r_2 \tag{12}$$

where r_1 and r_2 are distances from source and its image to the observation point.

2.3 Numerical solution

Applying the moment method techniques originated by Harrington [16], solution of (1) by matrix method leads to current distribution. The grounding system is first divided into N segments. Then the electric field E_m^s at the central point at the surface of the m^{th} conductor segment due to constant current I_n at the axis of the n^{th} segment is determined. The generalized impedance matrix may be constructed using (4):

$$Z_{mn} = -E_m^s \cdot \ell_m / I_n \tag{13}$$

Finally the unknown current distribution $[I]$ may be determined by solution of the matrix equation:

$$[Z] \cdot [I] = [Z'I_S] \tag{14}$$

where $[Z]$ is generalized impedance matrix and $[Z'I_S]$ is excitation matrix where I_S is current injected in the grounding system and Z' is impedance matrix between the segment in which the current I_S is injected and other segments [8].

When the current distribution is determined, the fields, potentials and voltages may be straightforwardly determined for frequencies in a range of interest for transient study [7,8]. Lastly, the time domain response may be obtained by Fourier or Laplace transform techniques [8] or by application of EMTP [9].

3. Validation

Figure 1 shows the oscillograms of the recorded current impulse injected at the end point of 15 meters long horizontal ground wire and transient voltage to remote ground at the same point. The electrode was constructed of a 116 mm^2 copper wire buried at 0.6 m depth in soil with resistivity 70 Ωm and relative permittivity 15 [13,17]. The simulation results show good consistency with the measurements.

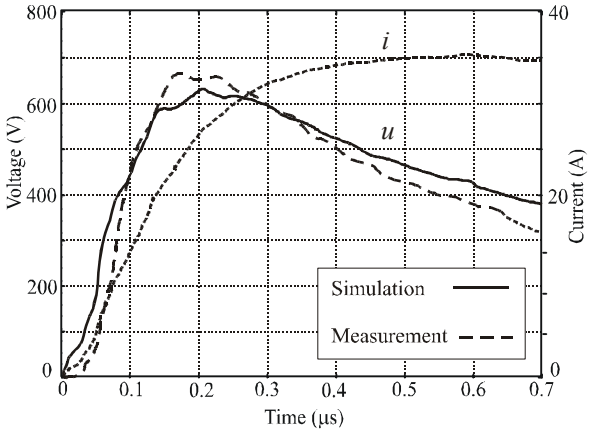

Fig. 1. Measurement and simulation of transient voltages to remote ground at the beginning point of 15 m long horizontal wire.

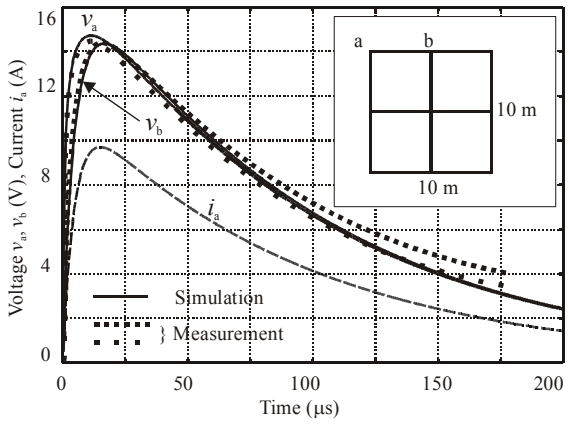

Fig. 2. Measurement and simulation of the voltages to remote ground at points *a* and *b* of 10 × 10 m^2 grounding grid.

Figure 2 shows results of a computer simulation for the ground grid measurements in [14]. The current is a double-exponential function (with T_1 / T_2 = 10 μs / 85 μs) matched to the measured one and the voltages to remote ground obtained

by the simulation are in good agreement with the measured ones.

4. Comparison between electromagnetic field and circuit models

In Fig. 3 circuit model [11] is compared with the electromagnetic model. The results at 50 Hz are in good agreement; while at 100 kHz there is large overestimate of the potentials in the circuit model. It could be expected that at 1 MHz this discrepancy of the results would be considerable larger. This is one example of a general conclusion that circuit models should not be applied for computation of field distributions at high frequencies.

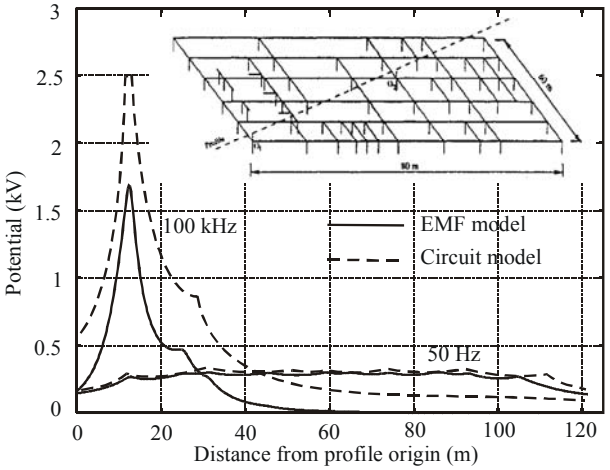

Fig. 3. Comparison of scalar potential along a profile at earth's surface above 80 × 60 m^2 grounding grid computed by circuit [11] and electromagnetic field models.

5. Analysis of the dynamic behavior to grounding grids

In this paper we analyze the spatial and temporal distributions of the scalar potential at the grounding grid conductors during the first part of the transient period when a lightning current impulse is injected into the grounding grid. Such distributions give an insight into the local inequalities of the reference voltages at different points of the grid. However, it should be emphasized that these distributions cannot be used to evaluate voltages between two points. The voltages in general are path dependent and should be calculated by integrating the electric field along a given path [8,20]. The voltages along different paths should be different if there is any time varying magnetic flux through the area bounded by these paths [19].

Computer software used for computations is shortly described in the Appendix.

5.1 Description of the cases adopted for computations

We consider three grounding grids constructed of copper conductors with diameter 1.4 cm, buried at 0.5 m depth (Fig. 4):

1. Type A: 60 m × 60 m with 6 by 6 10 m square meshes;
2. Type B: 60 m × 60 m with 10 by 10 6 m square meshes;
3. Type C: 120 m × 120 m with 10 by 10 12 m square meshes;

Two types of homogeneous soil are considered: "Resistive soil" with resistivity 1000 Ωm and relative permittivity 9 and "Conductive soil" with resistivity 100 Ωm and relative permittivity 36 .

Concerning the location of the feed point, two scenarios are considered: injection in the corner point, and, alternatively, in the center point of the grid. Also two shapes of the current impulse are considered. Both are usual "double-exponential" impulses with peak value 1 kA and time-to-half-maximum T_2 = 50 μs and two values of the time-to-maximum, the first one T_1 = 1 μs and second one T_2 = 5 μs:

$$i(t) = I\left(e^{-\alpha t} - e^{-\beta t}\right) \tag{15}$$

where the values of constants are:

1. T_1 / T_2 = 1 μs / 50 μs: I = 1.016 kA, a = 0.0142 μs^{-1}, b = 5.073 μs^{-1},
2. T_1 / T_2 = 5 μs / 50 μs: I = 1.043 kA, a = 0.0158 μs^{-1}, b = 0.800 μs^{-1}.

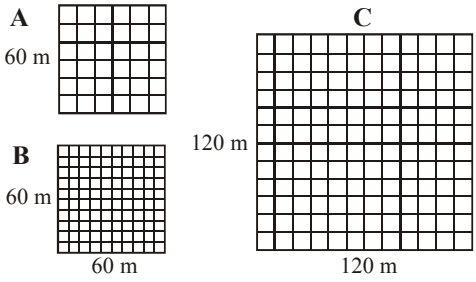

Fig. 4. Grounding Grids Adopted for Computations

5.2 Basic case for comparisons

Fig. 5 gives the "basic" case for comparisons. Grid A is buried in soil with ρ = 1000 Ωm and ε_r = 9 ("Resistive soil") subjected to 1/50 μs 1 kA current impulse injected in the corner. Distribution of potentials of grid conductors at three moments of time, during the rise of the injected current impulse, that is, at t = 0.1 μs, t = 0.5 μs, and t = 1 μs, are presented.

The maximum values of the potentials (of about 30 kV) are developed on conductors near the feed point around 0.2 μs, that is, earlier than the maximum of the excitation current impulse at 1 μs. From there potentials propagate over the grid conductors, until they are developed on the whole surface of the grid. The transient period is very short and can be estimated to 1.5 μs. After that time, potentials are equalized over the grid, i.e., distribution typical for DC excitation is developed.

5.3 Influence of the location of feed point

The case shown in Fig. 6 is the same as in the previous "basic case," except that the location of the feed point is in the center. The results in Fig. 6 show that the location of feed point has large influence on the maximum values of the potentials and on the duration of the transient period, leading to smaller potentials and shorter transient time. Maximum values are smaller and are only around 30% of the values in the "basic case" (around 10 kV). The maximums are developed at the same time as previously, at about 0.2 μs. The transient period is about 50% shorter than for injection in corner, that is, about 0.8 μs. This is related to the half shorter distance between the feed point and the edge of the grid and the same velocity of propagation of potentials over the grid conductors.

5.4 Influence of the soil resistivity

The case shown in Fig. 7 is the same as in the "basic case" except that the soil is with ρ = 100 Ωm and ε_r = 36 ("Conductive soil"). The results in Fig. 7 show that soil resistivity has exceptionally large influence on the transient potentials. In this case the maximum values are much smaller (less than 30% of the values in the "basic case"), but the duration of the transient period is much longer (around 10 times longer), compared to the "basic case" (Fig. 5). Maximum values are around 8 kV, developed at around 0.5 μs, and transient period

lasts up to about 15 μs. That means that the velocity by which potentials propagate over the grid conductors is approximately ten times smaller than in the previous cases.

5.5 Influence of the conductor separation

Illustration of the influence of the conductor separation is given in Fig. 8, which shows grid type B (Fig. 4) with all other parameters same as in the "basic case." The conductors in grid B are nearly double closer spaced than in grid A, since the meshes are nearly double smaller, 6 m × 6 m in comparison to 10 m × 10 m. This results in reduction of the potentials for about 15%, in comparison with the "basic case." Closer conductors have not significant influence on the other aspects of the transient process.

5.6 Influence of lightning current impulse front time

Fig. 9 illustrates the influence of the lightning current impulse front time which is five times longer: T_2 = 5 μs. The other parameters are same as in the "basic case." Impulse front time has large influence on the transient response: the maximum values are 50% smaller, they are developed at about 1 μs, and transient process lasts up to 5 μs.

5.7 Influence of the grid size

Fig. 10 illustrates the transient performance of 120 m × 120 m grid with 10 × 10 12 m square meshes: grid type C (Fig. 4). Results show that grid size does not influence the maximum values of the potentials, but it is the expected influence on the duration of the transient processes. Transient period is now double longer, because of the double larger dimensions of the grid.

6. Conclusion

The paper presents application of the electromagnetic field model for simulation of transients in spacious grounding grids. The model is validated by comparison with carefully documented independent experimental work. It has been demonstrated that existing more simplified circuit models could not be used for the same task.

Presented results indicate development of large transient potentials on the grounding grid conductors in the first moments after injection of lighting current impulse (results are normalized for 1 kA peak value of the lightning impulse).

The rise time of the transient potentials is shorter than the rise time of the lightning current impulse (for front time of the current impulse 1 μs, front time of the potentials is typically 0.2 μs). That indicate that the frequency content of the transient potentials is higher that the lightning current impulses.

The duration of the transient processes is short (from 1 μs to few tens μs for analyzed cases) and subsequently distribution typical for DC case is developed.

The parameter that has the greatest influence on the transient performance of the grid is:

- soil conductivity (for variation of the soil conductivity from 1000 Ωm to 100 Ωm, variation of voltage maximums is as 3:1 and transient period as 1:10),

The parameters that largely influence the transient performance of the grid are:

- location of feed point (for the variation of location of the feed point from center to corner of the grid, maximum values of the potentials are larger as 3:1 and the duration of the transient period is larger as 2:1), and,
- lightning current impulse front time (for variation of the impulse front time from 1 μs to 5 μs maximum values of the potentials are smaller as 1:2, but the duration of the transient processes is longer as 5:1).

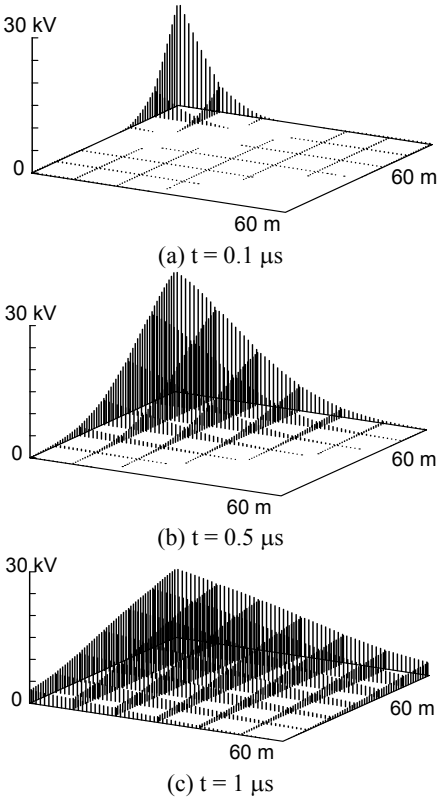

Fig. 5. Basic case for comparison: Grid type A; Injection in corner; "Resistive soil"; T_1 / T_2 = 1 μs / 50 μs with 1 kA crest current impulse.

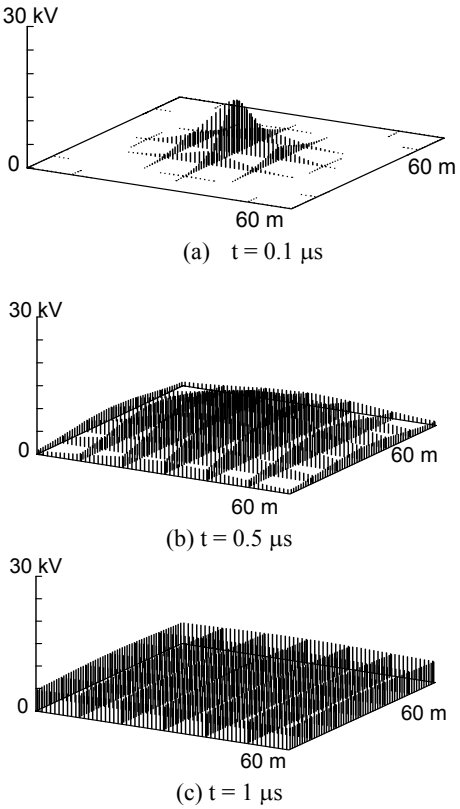

Fig. 6. Influence of the location of feed point: Injection in center.

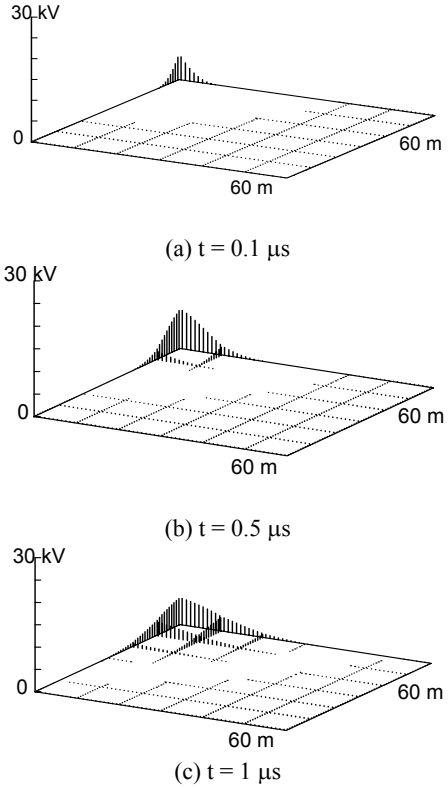

Fig. 7. Influence of the soil resistivity: "Conductive soil".

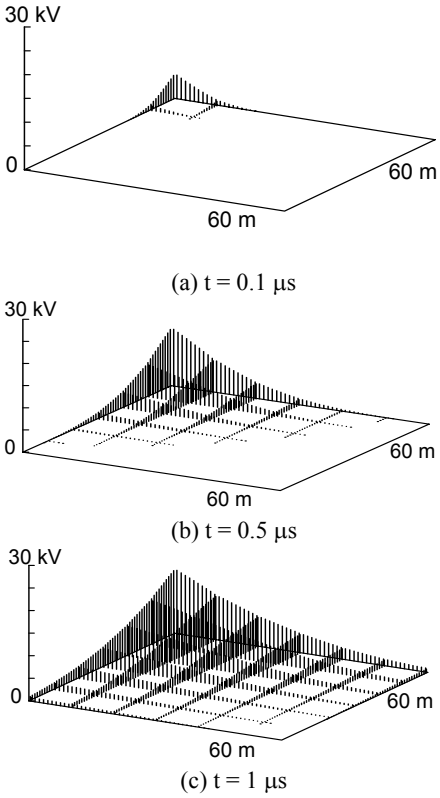

Fig. 9. Influence of the lightning current impulse front time: 5 μs / 50 μs 1kA Current impulse.

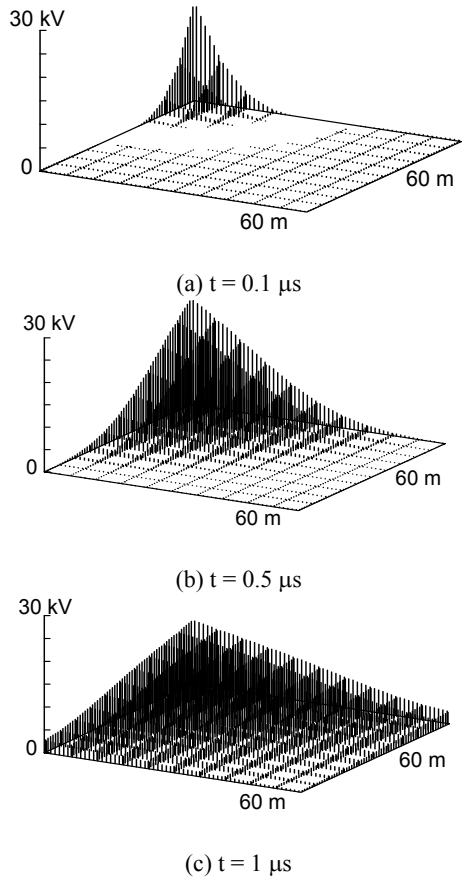

Fig. 8. Influence of conductor separation: Grid type B.

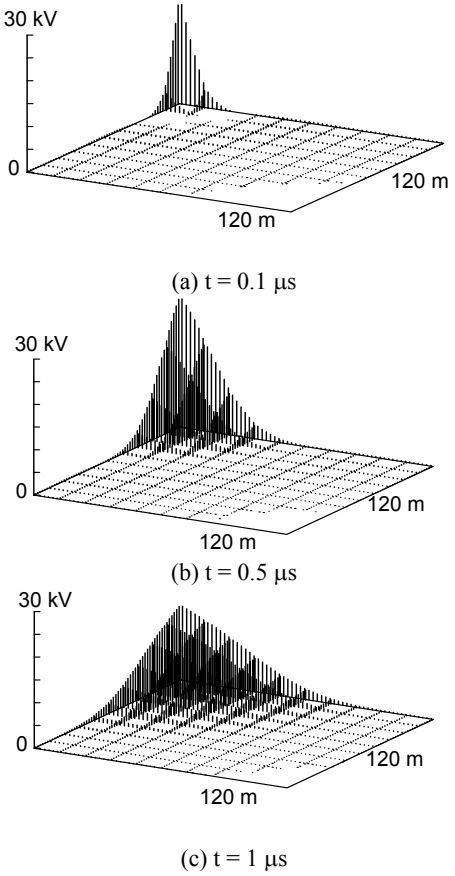

Fig. 10. Influence of the grid size: Grid type C.

The parameters that influence the transient response of the grid in smaller extent are:
- conductor separation (double closer separation reduce potentials in small extent (15%) and have no influence on the transient period),
- size (have no influence on the maximum values of the potentials, but in case of larger dimensions the transient period is longer).

7. Appendix – Short description of the computer software used for computations

Computations in this paper were made by TRAGSYS [18], a software package for high frequency and transient analysis of grounding systems for Windows.

7.1 Calculation method

TRAGSYS is aimed for computing the low and high frequency, and the transient behavior of grounding structures. It uses an antenna theory model based on a rigorous integral formulation derived from the complete set of Maxwell's equations. The solution is obtained in frequency-domain and the transient response by inverse Fourier transform techniques. Results are validated by comparison with independent field measurements and by comparison with other authors' models [8].

7.2 Input

Input data consists of: geometrical data of a network of connected or separated buried conductors with arbitrary orientation, conductivity of the conductors and characteristics of soil, and location and shape of injected current impulses. User-friendly input of data is enabled in graphical mode, which enables easy definition and modification of the geometry after viewing the results.

7.3 Output

Results of the computations are: impedance to ground, 3D perspectives or 2D plots of scalar potentials and/or electromagnetic fields, voltages along paths; all in frequency- and/or time-domain.

8. Acknowledgement

The author would like to thank Dr. A. P. J. van Deursen for his careful reading of the paper and for comments and suggestions that helped to improve the manuscript. The contributions to the Section 2 of this paper by Vesna Arnautovski-Toseva are gratefully acknowledged. The Ministry of Education and Science of the Republic of Macedonia sponsored in part the work reported in this paper.

9. References

[1] Vainer, A. L., "Impulse Characteristics of Complex Earthings," Electrichestvo, No. 3, 1966, pp. 23-27, (in Russian).

[2] Gupta, B. R.; Thapar, B., "Impulse Impedance of Grounding Grids," IEEE Trans. Power Apparatus and Systems, Vol. PAS-99, pp. 2357-2362, Nov./Dec. 1980.

[3] Verma, R.; Mukhedkar, D., "Fundamental Considerations and Impulse Impedance of Grounding Grids," IEEE Trans. Power Apparatus and Systems, Vol. PAS-100, pp. 1023-1030, March 1981.

[4] Meliopoulos, A. P.; Moharam, M.G., "Transient Analysis of Grounding Systems," IEEE Trans. Power Apparatus and Systems, Vol. PAS-102, pp. 389-399, Feb. 1983.

[5] Papalexopoulos, A. D.; Meliopoulos, A. P., "Frequency Dependent Characteristics of Grounding Systems," *IEEE Trans. Power Delivery*, Vol. PWRD-2, pp. 1073-1081, October 1987.

[6] Ramamoorty, M.; Narayanan, M. M. B.; Parameswaran, S.; Mukhedkar, D., "Transient Performance of Grounding Grids," *IEEE Trans. Power Delivery.*, Vol. PWRD-4, pp. 2053-2059, Oct. 1989.

[7] Grcev, L.; Dawalibi, F., "An Electromagnetic Model for Transients in Grounding Systems,'' *IEEE Trans. Power Delivery*, Vol. 5, pp. 1773-1781, No. 4, November 1990.

[8] Grcev, L. D., "Computer analysis of transient voltages in large grounding systems," *IEEE Trans. Power Delivery*, Vol. 11, No. 2, April 1996, pp. 815-823

[9] Heimbach, M.; Grcev, L.D., "Grounding system analysis in transients programs applying electromagnetic field approach," *IEEE Trans. Power Delivery*, Vol. 12, No. 1, Jan. 1997, pp. 186-193.

[10] Geri, A., "Behaviour of grounding systems excited by high impulse currents: the model and its validation," *IEEE Trans. Power Delivery*, Vol. 14, No. 3, July 1999, pp. 1008 –1017.

[11] Otero, A.F.; Cidras, J.; del Alamo, J.L., "Frequency-dependent grounding system calculation by means of a conventional nodal analysis technique," *IEEE Trans. Power Delivery*, Vol. 14, No. 3, July 1999, pp. 873 –878.

[12] Yaqing Liu; Zitnik, M.; Thottappillil, R., "An improved transmission-line model of grounding system," *IEEE Trans. Electromagnetic Compatibility*, Vol. 43, No. 3, Aug. 2001, pp. 348 –355.

[13] Saint-Privat-d'Allier Research Group, "Eight Years of Lightning Experiments at Saint-Privat-d'Allier," *Review Generale de l'Electricite (RGE)*, Vol. 91, September 1982, pp. 561-582.

[14] Stojkovic, Z.; Savic, M.S.; Nahman, J.M.; Salamon, D.; Bukorovic, B., "Sensitivity analysis of experimentally determined grounding grid impulse characteristics", *IEEE Transactions on Power Delivery*, Vol. 13, No. 4, Oct. 1998, pp. 1136 –1142.

[15] Bickford, J. P.; Mullineux, N.; Reed, J. R., *Computation of power system transients*, London: IEE, 1976.

[16] Harrington, R.F., *Field computation by moment methods*, New York: IEEE Press, 1993.

[17] Rochereau, H., "Application of the Transmission Lines Theory and EMTP Program for Modelisation of Grounding Systems in High Frequency Range", Collection de notes internes de la Direction des Etudes et Recherches, 93NR00059, 1993.

[18] CIGRÉ WG 36.04, *Guide on Electromagnetic Compatibility in Electric Power Plants and Substations*, Publication No. 124, CIGRÉ, Paris, 1997.

[19] Ramo, S.; Whinnery, J. R.; van Duzer, T., *Fields and waves in communication electronics*, 3rd Ed., New York: Wiley, 1994.

[20] L. Grcev, "Transient Voltages Coupling to Shielded Cables Connected to Large Substations Earthing Systems due to Lightning," 1996 CIGRE Session, (Paper 36-201).